Energy Conversion and Management 52 (2011) 15–26

Contents lists available at ScienceDirect

Energy Conversion and Management

journal homepage: www.elsevier.com/locate/enconman

Probability distributions for offshore wind speeds

Eugene C. Morgan [a,*], Matthew Lackner [b], Richard M. Vogel [a], Laurie G. Baise [a]

[a] Dept. of Civil and Environmental Engineering, Tufts University, 200 College Ave., Medford, MA 02155, United States
[b] Wind Energy Center, University of Massachusetts, Amherst, United States

ARTICLE INFO

Article history:
Received 30 September 2009
Accepted 2 June 2010
Available online 14 July 2010

Keywords:
Wind speed
Probability distribution
Mixture distribution
Wind turbine energy output
Weibull distribution
Extreme wind

ABSTRACT

In planning offshore wind farms, short-term wind speeds play a central role in estimating various engineering parameters, such as power output, extreme wind load, and fatigue load. Lacking wind speed time series of sufficient length, the probability distribution of wind speed serves as the primary substitute for data when estimating design parameters. It is common practice to model short-term wind speeds with the Weibull distribution. Using 10-min wind speed time series at 178 ocean buoy stations ranging from 1 month to 20 years in duration, we show that the widely-accepted Weibull distribution provides a poor fit to the distribution of wind speeds when compared with more complicated models. We compare distributions in terms of three different metrics: probability plot R^2, estimates of average turbine power output, and estimates of extreme wind speed. While the Weibull model generally gives larger R^2 than any other 2-parameter distribution, the bimodal Weibull, Kappa, and Wakeby models all show R^2 values significantly closer to 1 than the other distributions considered (including the Weibull), with the bimodal Weibull giving the best fits. The Kappa and Wakeby distributions fit the upper tail (higher wind speeds) of a sample better than the bimodal Weibull, but may drastically over-estimate the frequency of lower wind speeds. Because the average turbine power is controlled by high wind speeds, the Kappa and Wakeby estimate average turbine power output very well, with the Kappa giving the least bias and mean square error out of all the distributions. The 2-parameter Lognormal distribution performs best for estimating extreme wind speeds, but still gives estimates with significant error. The fact that different distributions excel under different applications motivates further research on model selection based upon the engineering parameter of interest.

1. Introduction

The offshore environment shows greater wind energy potential than most terrestrial locations [1]. Accurate characterization of offshore winds will be essential in tapping this tremendous power source. In wind turbine design and site planning, the probability distribution of short-term wind speed becomes critically important in estimating energy production. Here short-term wind speed U refers to mean wind speed averaged on the time scale of 10 min, which is much longer than the time scale associated with turbulence and gusts. In engineering practice, the average wind turbine power $\overline{P}_w$ associated with the probability density function (pdf) of wind speeds U is obtained from

$$\widehat{\overline{P}}_w = \int_0^\infty P_w(U) f(U) dU, \tag{1}$$

where $f(U)$ is the pdf of U and where the turbines power curve $P_w(U)$ describes power output versus wind speed [2]. The largest uncertainty in the estimation of $\overline{P}_w$ lies in the choice of the wind speed pdf $f(U)$, since the turbine manufacturer knows $P_w(U)$ fairly accurately. Minimizing uncertainty in wind resource estimates greatly improves results in the site assessment phase of planning [3], and this can be accomplished by utilizing a more accurate distribution (pdf).

By far the most widely-used distribution for characterization of 10-min average wind speeds is the 2-parameter Weibull distribution (W2) [2,4–9]. Sometimes the simple 1-parameter Rayleigh (RAY) distribution offers a more concise fit to a sample, since it is a special case of the W2 [2,10], but ultimately having only a single model parameter makes the RAY much less flexible. Despite the widespread acceptance of the W2 and RAY distributions, Carta et al. [11] and others have noted that under different wind regimes other distributions may fit wind samples better. Other distributions used to characterize wind speed include the 3-parameter Generalized Gamma (GG), 2-parameter Gamma (G2), inverse Gaussian, 2-parameter Lognormal (LN2), 3-parameter Beta, singly truncated from below Normal, distributions derived from the Maximum Entropy Principle, and bimodal (two component mixture) Weibull model (BIW). Kiss and Janosi [12] recommend the GG for the ERA-40 dataset (6-hourly mean) after testing the RAY, W2

* Corresponding author. Tel.: +1 617 627 3098.
E-mail address: eugene.morgan@tufts.edu (E.C. Morgan).

0196-8904/$ - see front matter © 2010 Elsevier Ltd. All rights reserved.
doi:10.1016/j.enconman.2010.06.015

and LN2 distributions. Simiu et al. [13] use probability plot correlation coefficient (PPCC) goodness-of-fit tests to document that the RAY distribution provides a poor approximation to hourly wind speeds, but the authors do not advocate an alternative.

Recent studies show that Weibull mixture models (including BIW) out-perform the W2 distribution [14–16]. However, these studies only use a limited number of samples from confined geographic regions, and often explain the better fits of the mixture models as unique exceptions to the rule. For example, Akpinar and Akpinar [15] show that mixture models out-perform the Weibull distribution and other distributions derived from the Maximum Entropy Principle, but only use 4 samples from a single region in Turkey. Carta and Ramirez [16] arrive at similar findings for 16 samples in the Canary Islands, as do Jaramillo and Borja [14] for one sample from La Ventosa, Mexico.

One goal of this study is to exploit a much larger and geographically diverse dataset than previous studies in order to evaluate alternative wind speed distributional hypotheses, such as the BIW model. We use data spread out over many different wind regimes, albeit all from ocean environments, in order to assess the communicability of such models. While the offshore setting for all samples in this study may limit the utility of some of our findings for onshore data, we find the use of this data essential in removing topographic effects, which would complicate a similar analysis performed on terrestrial wind speed samples.

Another primary goal of this study is to illustrate that finding an optimal wind speed distributional model is contingent upon the application of interest. Measures of goodness-of-fit commonly used in wind literature (i.e. R^2) [17,16,18,12,10,5,11] do not necessarily indicate how well a model predicts wind energy parameters. Following Chang and Tu [19], a model validation approach based on parameter estimation instead of R^2 may find theoretical models that are best suited for specific wind energy applications. In practice, one may resort to a variety of models to give optimal predictions of in situ conditions when lacking observations.

2. Data

The National Data Buoy Center (NDBC) [20] provides 10-min mean wind speed observations recorded at 178 buoys around North America (Fig. 1). We analyze the 10-min mean wind speed data because the International Electrotechnical Commission requires the evaluation of this form of wind measurement in turbine site assessment [21]. Depending on the type of buoy, the anemometers on the buoys measure wind speed at either 5 or 10 m above sea level. Sample sizes (n) range from 4,314 to 889,699, corresponding to time spans of approximately 30 days to 20 years. This dataset comprises the largest collection of first-order wind speed observations that we could find readily available online and that provides a relatively reliable and consistent measurement of short-term wind speeds.

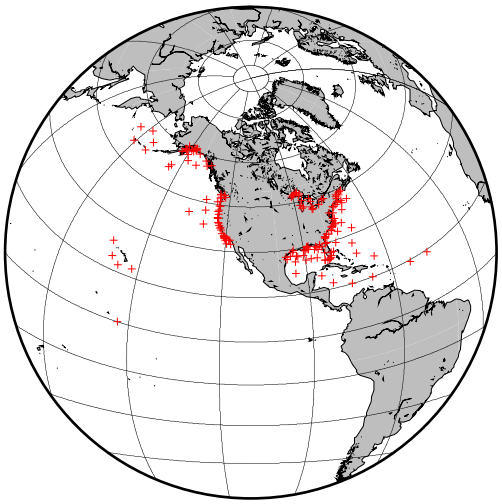

Fig. 1. Locations of buoys providing wind speed observations for this study. Data source: http://www.ndbc.noaa.gov.

3. Wind speed distributions

We consider some of the most common wind speed distributions used in previous studies. We also consider numerous other closely-related distributions, such as the Generalized Rayleigh (GR), Kappa (KAP), and Wakeby (WAK) distributions, that have not previously been investigated as wind speed models, but are simple extensions or generalizations of commonly used models. The 2-parameter GR distribution is a generalization of the 1-parameter RAY distribution, and the KAP and WAK distributions (with four and five parameters, respectively) are generalizations of numerous other distributions.

Since the record lengths of the time series of wind speeds are rather large, differences among parameter estimation methods will not be nearly as important as differences among distributions. We preferentially use maximum likelihood estimators (MLE) because they usually yield lower mean square errors (MSE) associated with model parameter estimates than method of moments (MOM) estimators for the large samples considered here. However, for some distributions we use MOM, least squares (LS), or a parameter estimation method involving L-moments when MLEs are either too cumbersome or unavailable, as discussed in each case. When using MOM, we calculate the sample mean ($\overline{U}$), standard deviation (S), and skewness (G) as

$$\overline{U} = \frac{1}{n}\sum_{i=1}^{n} U_i, \tag{2}$$

$$S = \sqrt{\frac{1}{n-1}\sum_{i=1}^{n}(U_i - \overline{U})^2}, \tag{3}$$

$$G = \frac{1}{n}\frac{\sum_{i=1}^{n}(U_i - \overline{U})^3}{S^3}, \tag{4}$$

where n is the number of observations in U, our random variable for wind speed. The following describes each distribution in our study and the parameter estimation methods used.

3.1. Rayleigh

The Rayleigh (RAY) distribution is the simplest distribution commonly used to describe 10-min average wind speeds [2,4,17] because it only has a single model parameter b. Its pdf $f(U)$, and cumulative distribution function (cdf) $F(U)$, are

$$f(U;b) = \frac{U}{b^2}\exp\left(-\frac{1}{2}\frac{U^2}{b^2}\right), \tag{5}$$

and

$$F(U;b) = 1 - \exp\left(-\frac{1}{2}\frac{U^2}{b^2}\right), \tag{6}$$

for $U \geqslant 0$ and $b \geqslant 0$. We estimate the single scale parameter b using the MLE:

$$\hat{b} = \sqrt{\frac{1}{2n}\sum_{i=1}^{n} U_i^2}. \tag{7}$$

Often databases report wind speeds as two orthogonal components (u and v). If u and v are independent and identically distributed Gaussian random variables with means of zero and standard deviations of b^2, $U = \sqrt{u^2 + v^2}$ follows a Rayleigh distribution [22]. However, NDBC does not report wind speeds in separate u, v components.

3.2. Weibull

The Weibull (W2) distribution constitutes the most widely accepted distribution for wind speed [2,4–9]. It is a generalization of the RAY distribution, and has been shown to fit wind samples better than RAY due to its more flexible form (with an additional shape parameter) [17,12]. The Weibull pdf and cdf are

$$f(U;\beta,\alpha) = \frac{\beta U^{\beta-1}}{\alpha^{\beta}} \exp\left[-\left(\frac{U}{\alpha}\right)^{\beta}\right], \tag{8}$$

and

$$F(U;\beta,\alpha) = 1 - \exp\left[-\left(\frac{U}{\alpha}\right)^{\beta}\right], \tag{9}$$

with $U \geqslant 0$. The RAY is a special case of the W2 with $\beta = 2$ [23]. MLEs are obtained by solving

$$\frac{\sum_{i=1}^{n}\left(U_i^{\hat{\beta}} \ln U_i\right)}{\sum_{i=1}^{n} U_i^{\hat{\beta}}} - \frac{1}{\hat{\beta}} - \frac{1}{n}\sum_{i=1}^{n} \ln U_i = 0 \tag{10}$$

iteratively for the shape parameter estimate $\hat{\beta}$, and then using

$$\hat{\alpha} = \left(\frac{1}{n}\sum_{i=1}^{n} U_i^{\hat{\beta}}\right)^{\frac{1}{\hat{\beta}}} \tag{11}$$

for the scale parameter estimate $\hat{\alpha}$.

3.3. Generalized Rayleigh

Another generalization of the RAY distribution is the generalized Rayleigh (GR) model, which is sometimes referred to as the 2-parameter Burr Type X distribution [24]. While the GR has not previously been applied to wind speed samples, it is a natural extension of the RAY distribution (like the W2 distribution). It has a pdf

$$f(U;\alpha,\lambda) = 2\alpha\lambda^2 U \exp[-(\lambda U)^2](1 - \exp[-(\lambda U)^2])^{\alpha-1}, \tag{12}$$

and cdf

$$F(U;\alpha,\lambda) = (1 - \exp[-(\lambda U)^2])^{\alpha}, \tag{13}$$

for $U > 0$. We estimate the shape α and scale λ parameters using the modified moment estimators introduced by Kundu and Raqab [24]:

$$W = \frac{1}{n}\sum_{i=1}^{n} U_i^2, \tag{14}$$

$$V = \frac{1}{n}\sum_{i=1}^{n} U_i^2 - W^2, \tag{15}$$

$$\frac{V}{W^2} = \frac{\psi'(1) - \psi'(\hat{\alpha}+1)}{(\psi(\hat{\alpha}+1) - \psi(1))^2}, \tag{16}$$

which requires solving iteratively for $\hat{\alpha}$, and

$$\hat{\lambda} = \sqrt{\frac{\psi(\hat{\alpha}+1) - \psi(1)}{W}}, \tag{17}$$

where $\psi()$ is the digamma function and $\psi'()$ is the polygamma function of order one.

3.4. 3-parameter Weibull

The 3-parameter Weibull (W3) is a generalization of the W2 distribution, where the location parameter τ establishes a lower bound (which was assumed to be zero for the W2 distribution). Stewart and Essenwanger [25] found that the W3 fits wind speed data better than the W2 model. The W3 pdf and cdf are

$$f(U;\beta,\alpha,\tau) = \frac{\beta U^{\beta-1}}{\alpha^{\beta}} \exp\left[-\left(\frac{U-\tau}{\alpha}\right)^{\beta}\right], \tag{18}$$

and

$$F(U;\beta,\alpha,\tau) = 1 - \exp\left[-\left(\frac{U-\tau}{\alpha}\right)^{\beta}\right], \tag{19}$$

respectively, for $U \geqslant \tau$. We estimate the parameters using the modified MLEs recommended by Cohen [26]:

$$\frac{\sum_{i=1}^{n}(U_i - \hat{\tau})^{\hat{\beta}} \ln(U_i - \hat{\tau})}{\sum_{i=1}^{n}(U_i - \hat{\tau})^{\hat{\beta}}} - \frac{1}{\hat{\beta}} - \frac{1}{n}\sum_{i=1}^{n} \ln(U_i - \hat{\tau}) = 0, \tag{20}$$

$$\hat{\alpha} = \left(\frac{1}{n}\sum_{i=1}^{n}(U_i - \hat{\tau})^{\hat{\beta}}\right)^{\frac{1}{\hat{\beta}}}, \tag{21}$$

$$\hat{\tau} + \frac{\hat{\alpha}}{n^{\frac{1}{\hat{\beta}}}}\Gamma\left(1 + \frac{1}{\hat{\beta}}\right) = U_1, \tag{22}$$

where n is the number of observations in sample U, and U_1 indicates the minimum value of U. First, $\hat{\tau}$ is found by iteratively solving Eqs. (20)–(22), and then $\hat{\beta}$ is found by iteratively solving Eq. (20). Finally, $\hat{\alpha}$ is given by Eq. (21) using the estimates of the other two parameters [23,26].

3.5. Lognormal

The 2-parameter Lognormal (LN2) pdf and cdf are

$$f(U;\mu,\sigma) = \frac{1}{\sigma U\sqrt{2\pi}} \exp\left[\frac{-(\ln(U) - \mu)^2}{2\sigma^2}\right], \tag{23}$$

and

$$F(U;\mu,\sigma) = \frac{1}{2} + \frac{1}{2}\mathrm{erf}\left[\frac{\ln(U) - \mu}{\sigma\sqrt{2}}\right], \tag{24}$$

where erf() is the error function from the Normal distribution, and the parameters μ and σ are the mean and standard deviation of the natural logarithm of U [5,12,17,27]. Since some observations may be zero, we employ MOM estimators [28] instead of MLEs as follows:

$$\hat{\mu} = \ln\left(\frac{\overline{U}}{\sqrt{1 + \frac{S^2}{\overline{U}^2}}}\right), \tag{25}$$

$$\hat{\sigma} = \sqrt{\ln\left(1 + \frac{S^2}{\overline{U}^2}\right)}. \tag{26}$$

For both the 2- and 3-parameter Lognormal distributions, we chose MOM over MLE because it showed considerably better fits to the data and because it enables us to handle samples with zeros. The results of Carta et al. [17] corroborate this statement with short-term wind speed observations from the Canary Islands, showing that MOM for LN2 fits the data better than MLE for 5 of 8 samples.

3.6. 3-parameter Lognormal

The 3-parameter Lognormal (LN3) model is a shifted version of the LN2, with pdf

$$f(U;\mu,\sigma,\zeta)=\frac{1}{\sigma U\sqrt{2\pi}}\exp\left[\frac{-(\ln(U-\zeta)-\mu)^2}{2\sigma^2}\right], \tag{27}$$

and cdf

$$F(U;\mu,\sigma)=\frac{1}{2}+\frac{1}{2}\mathrm{erf}\left[\frac{\ln(U-\zeta)-\mu}{\sigma\sqrt{2}}\right], \tag{28}$$

where the location parameter ζ establishes a lower bound on the distribution. This distribution has yet to be fit to wind speeds, but we expect it to perform as well or better than the LN2 model. MOM estimates the three parameters via the following equations:

$$\exp[\hat{\sigma}^2]=\left(1+\frac{1}{2}\left[G^2+G(4+G^2)^{\frac{1}{2}}\right]\right)^{\frac{1}{3}}+\left(1+\frac{1}{2}\left[G^2-G(4+G^2)^{\frac{1}{2}}\right]\right)^{\frac{1}{3}}-1, \tag{29}$$

$$\hat{\mu}=\frac{1}{2}\ln\left(\frac{S^2}{\exp(\hat{\sigma}^2)[\exp(\hat{\sigma}^2)-1]}\right), \tag{30}$$

$$\hat{\zeta}=\overline{U}-\exp\left(\hat{\mu}+\frac{1}{2}\hat{\sigma}^2\right), \tag{31}$$

which allow us to keep null values ($U=0$) [28].

3.7. Generalized Normal

The Generalized Normal (GNO) model encompasses Lognormal distributions with both positive and negative skewness, as well as the Normal distribution [29]. We consider this pdf due to its more general form than the LN2 pdf, which has previously been recommended for use with wind speed data [5,12,17,27]. The pdf and cdf are

$$y=\begin{cases}-k^{-1}\ln(1-k(U-\xi)/\alpha), & k\neq 0\\ (U-\xi)/\alpha, & k=0\end{cases}, \tag{32}$$

$$f(U;\alpha,k,\xi)=\frac{\exp(ky-y^2/2)}{\alpha\sqrt{2\pi}}, \tag{33}$$

and

$$F(U;\alpha,k,\xi)=\Phi(y), \tag{34}$$

where $\Phi()$ is the standard Normal cdf. The location ξ, scale α, and shape k parameters relate to standard parameters for the LN2 and LN3 distributions above by

$$k=-\sigma, \tag{35}$$

$$\alpha=\sigma\exp(\mu), \tag{36}$$

and

$$\xi=\zeta+\exp(\mu), \tag{37}$$

and we estimate these parameters using sample L-moments λ_1 and λ_2 and the sample L-moment ratio τ_3:

$$\hat{k}\approx-\tau_3\frac{2.0466-3.6544\tau_3^2+1.8397\tau_3^4-0.2036\tau_3^6}{1-2.0182\tau_3^2+1.242\tau_3^4-0.21742\tau_3^6}, \tag{38}$$

$$\hat{\alpha}=\frac{\lambda_2\hat{k}\exp(-\hat{k}^2/2)}{1-2\Phi\left(-\hat{k}/\sqrt{2}\right)}, \tag{39}$$

$$\hat{\xi}=\lambda_1-\frac{\hat{\alpha}}{\hat{k}}(1-\exp(\hat{k}^2/2)). \tag{40}$$

Hosking and Wallis [29] present this distribution, as well as an explanation of the sample L-moments and their ratios.

3.8. Gamma

The 2-parameter Gamma (G2) distribution has been applied to wind speed data by Sherlock [30], Kaminsky [27], and Auwera et al. [31], for example. This distribution is often referred to as a Pearson Type III, however in this paper we make a distinction between the two distributions in order to evaluate the effect of the added location parameter which we include in the Pearson Type III (P3). The G2 pdf and cdf are

$$f(U;\beta,\alpha)=U^{\alpha-1}\frac{\exp\left(-\frac{U}{\beta}\right)}{\beta^{\alpha}\Gamma(\alpha)}, \tag{41}$$

and

$$F(U;\beta,\alpha)=\gamma\left(\alpha,\frac{U}{\beta}\right)\Big/\Gamma(\alpha), \tag{42}$$

where $\gamma()$ is the lower incomplete gamma function [22]. In order to keep null wind speeds in the sample, we estimate the shape α and scale β parameters via MOM:

$$\hat{\beta}=\frac{S^2}{\overline{U}}, \tag{43}$$

$$\hat{\alpha}=\frac{\overline{U}^2}{S^2} \tag{44}$$

as given by Carta et al. [17]. Again, we do not use the MLEs for this distribution because they require removing all $U_i=0$.

3.9. Pearson type III

The Pearson type III (P3) distribution is a G2 distribution with a third parameter for location, whose use for wind speed was initially advocated by Putnam [32]. Its pdf and cdf are

$$f(U;\tau,\beta,\alpha)=(U-\tau)^{\alpha-1}\frac{\exp\left(-\frac{U-\tau}{\beta}\right)}{\beta^{\alpha}\Gamma(\alpha)}, \tag{45}$$

and

$$F(U;\tau,\beta,\alpha)=\gamma\left(\alpha,\frac{U-\tau}{\beta}\right)\Big/\Gamma(\alpha). \tag{46}$$

Again, to enable us to handle null wind speeds, we estimate the location τ, scale β, and shape α parameters using MOM [33]:

$$\hat{\tau}=\overline{U}-2\left(\frac{S}{G}\right), \tag{47}$$

$$\hat{\beta}=\frac{SG}{2}, \tag{48}$$

$$\hat{\alpha}=\frac{4}{G^2}. \tag{49}$$

The MLEs for this distribution require the removal of null wind speeds [34].

3.10. Log Pearson type III

The log Pearson type III (LP3) distribution describes a random variable whose logarithms follow a P3 distribution [33]. Thus, we fit the LP3 distribution to the wind speed sample U by transforming U by the natural logarithm and fitting the P3 distribution. The LP3 distribution is one of the most flexible 3-parameter distributions that exists. Thus, we sought to evaluate its performance, even though we could not find any previous studies which evaluate its use for wind speeds.

3.11. Generalized Gamma

The 3-parameter generalized Gamma (GG) distribution includes the W2, P3, and other distributions as special cases, and has been proposed as a wind speed model by several authors [12,17,31]. Its pdf and cdf are

$$f(U;\beta,\alpha,p) = |p|U^{p\alpha-1}\frac{\exp\left(-\frac{U}{\beta}\right)^p}{\beta^{p\alpha}\Gamma(\alpha)}, \tag{50}$$

and

$$F(U;\beta,\alpha,p) = \gamma\left(\alpha,\left(\frac{U}{\beta}\right)^p\right). \tag{51}$$

In order to avoid removing null wind speeds from the samples before fitting the model (as required by the MLEs), we estimate the scale β and shape parameters α, p by MOM. First, we solve the following equation iteratively for $\hat{\alpha}$:

$$-|G| = \psi''(\hat{\alpha})/(\psi'(\hat{\alpha}))^{3/2}, \tag{52}$$

and then find the remaining parameters with the following equations:

$$\hat{p} = (\psi'(\hat{\alpha}))^{1/2}/S, \tag{53}$$

$$\hat{\beta} = \exp(\overline{U} - \psi(\hat{\alpha})/\hat{p}), \tag{54}$$

where $\psi()$ is the digamma function, and $\psi'()$ and $\psi''()$ are the polygamma functions of order one and two [35].

3.12. Kappa

The 4-parameter Kappa (KAP) distribution is a generalization of many other distributions and includes as special cases the Generalized Logistic, Generalized Extreme Value, and Generalized Pareto distributions [29]. Its pdf and cdf are

$$f(U;\xi,\alpha,k,h) = \alpha^{-1}(1-k(U-\xi)/\alpha)^{1/k-1}(F(U))^{1-h}, \tag{55}$$

and

$$F(U;\xi,\alpha,k,h) = (1-h(1-k(U-\xi)/\alpha)^{1/k})^{1/h}, \tag{56}$$

respectively. We estimate the location ξ, scale α, and two shape parameters k, h by solving the following relationships between these parameters and the sample L-moments λ_1, λ_2 and L-moment ratios τ_3, τ_4:

$$\lambda_1 = \hat{\xi} + \hat{\alpha}(1-g_1)/\hat{k}, \tag{57}$$

$$\lambda_2 = \hat{\alpha}(g_1-g_2)/\hat{k}, \tag{58}$$

$$\tau_3 = (-g_1+3g_2-2g_3)/(g_1-g_2), \tag{59}$$

$$\tau_4 = (-g_1+6g_2-10g_3+5g_4)/(g_1-g_2), \tag{60}$$

where

$$g_r = \begin{cases} \frac{r\Gamma(1+\hat{k})\Gamma(r/\hat{h})}{\hat{h}^{1+\hat{k}}\Gamma(1+\hat{k}+r/\hat{h})}, & \hat{h}>0 \\ \frac{r\Gamma(1+\hat{k})\Gamma(-\hat{k}-r/\hat{h})}{(-\hat{h})^{1+\hat{k}}\Gamma(1-r/\hat{h})}, & \hat{h}<0 \end{cases}. \tag{61}$$

Given τ_3 and τ_4, we solve Eqs. (57) and (58) iteratively for $\hat{k}$ and $\hat{h}$ [29].

3.13. Wakeby

The 5-parameter Wakeby (WAK) distribution is a generalization of many existing pdfs (including LN2 and P3), but the WAK pdf can exhibit shapes that other distributions cannot mimic [36]. It has been considered as a super population or parent distribution in many previous studies in the earth sciences [37,38] and was originally introduced by Harold Thomas [39,40] who lived on Wakeby pond on Cape Cod. The pdf and cdf are not explicitly defined, and the WAK distribution is most easily defined by its quantile function:

$$F^{-1}(F(U);\xi,\alpha,\beta,\gamma,\delta) = \xi + \frac{\alpha}{\beta}(1-(1-F(U))^{\beta}) - \frac{\gamma}{\delta}(1-(1-F(U))^{-\delta}). \tag{62}$$

Parameter estimation follows an algorithm outlined in Hosking and Wallis [29] and Hosking [41] which relies on sample L-moments. We implement this distribution and its parameter estimation using the package *lmomco* [42] for the statistical software *R* [43].

3.14. Bimodal Weibull mixture

The bimodal Weibull mixture distribution (BIW) is a mixture of two W2 distributions. The BIW model exhibits two different modes and has been recommended for use with wind speed data by Carta et al. [17], Akpinar and Akpinar [15], Carta and Ramirez [18], and Jaramillo and Borja [14]. The pdf and cdf are

$$f(U;\beta_1,\alpha_1,\beta_2,\alpha_2,\omega) = \omega\frac{\beta_1 U^{\beta_1-1}}{\alpha_1^{\beta_1}}\exp\left[-\left(\frac{U}{\alpha_1}\right)^{\beta_1}\right] + (1-\omega)\frac{\beta_2 U^{\beta_2-1}}{\alpha_2^{\beta_2}}\exp\left[-\left(\frac{U}{\alpha_2}\right)^{\beta_2}\right], \tag{63}$$

and

$$F(U;\beta_1,\alpha_1,\beta_2,\alpha_2,\omega) = \omega\left(1-\exp\left[-\left(\frac{U}{\alpha_1}\right)^{\beta_1}\right]\right) + (1-\omega)\left(1-\exp\left[-\left(\frac{U}{\alpha_2}\right)^{\beta_2}\right]\right), \tag{64}$$

where the shape β and scale α parameters have subscripts corresponding to the two different modes, and the mixing parameter ω describes the proportion of observations belonging to the first component. We first estimate β_1 and α_1 using the MLE for the W2, and assign $\beta_2 = 1$, $\alpha_2 = 1$, and $\omega = 0.5$. Then, using these estimations as our initial parameters, we optimize the five parameters to give the LS fit of the model cdf to the empirical (wind sample) cdf. The least squares method is usually applied to the cdf [17].

4. Results and discussion

We evaluate the goodness-of-fit of the various fitted distributions to the buoy wind speed samples using the coefficients of determination associated with the resulting P–P probability plots, an example of which is presented in Fig. 2. R^2 is used widely for goodness-of-fit comparisons and hypothesis testing because it quantifies the correlation between the observed probabilities and the predicted probabilities from a distribution. Here we employ P–P probability plots instead of Q–Q probability plots (which plot predicted quantiles versus observed quantiles) because P–P plots do not require specially designed quantile unbiased plotting positions for each pdf considered. Instead, we use the Weibull plotting position $F(U) = i/(n+1)$, where i=1,..., n, in all cases because it always gives an unbiased estimate of the observed cumulative probabilities regardless of the underlying distribution considered, and does not estimate the highest observed wind speed as the maximum possible wind speed (i.e. $F(U_n) \neq 1$).

A larger value of R^2 indicates a better fit of the model cumulative probabilities $\widehat{F}$ to the empirical cumulative probabilities F. We determine R^2 as:

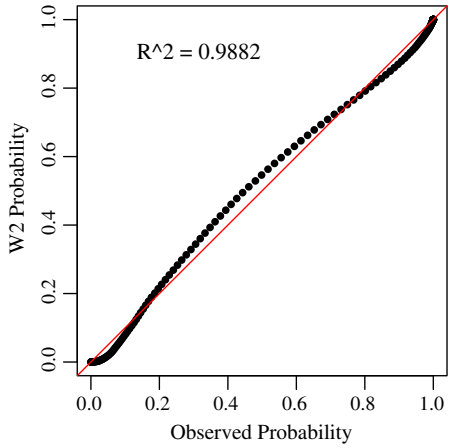

Fig. 2. Example P–P probability plot from buoy 41040. Red line denotes a 1:1 relationship between the model-predicted probabilities and the observed probabilities (i.e. $R^2 = 1$). (For interpretation of the references to colour in this figure legend, the reader is referred to the web version of this article.)

$$R^2 = \frac{\sum_{i=1}^{n}(\widehat{F}_i - \overline{F})^2}{\sum_{i=1}^{n}(\widehat{F}_i - \overline{F})^2 + \sum_{i=1}^{n}(F_i - \widehat{F}_i)^2}, \tag{65}$$

where $\overline{F} = \frac{1}{n}\sum_{i=1}^{n}\widehat{F}_i$. The estimated cumulative probabilities $\widehat{F}$ are obtained from the various models' cdfs described previously. We chose R^2 as the goodness-of-fit measure for ease of comparison between distributions, and also because of its widespread use in similar studies [5,17,44].

Fig. 3 ranks the distributions (from left to right) in terms of their goodness-of-fit as measured by their median R^2 values. Although the W2, the most widely accepted distribution for modeling wind speeds, performs the best out of all 2-parameter distributions and even better than some three-parameter distributions, it is not the model with the best goodness-of-fit in terms of R^2. The BIW, KAP, and WAK all show significant improvement in fit over the other pdfs, with the BIW exhibiting the highest R^2 values and the highest median R^2. In comparison to the WAK, the BIW model exhibits a wider variability in R^2 values and lower R^2 values for the poorly fit sites.

4.1. The probability distribution of offshore wind speeds

The poor performance of the W2 distribution for these samples compared to some of the more complex models can be further explained using moment diagrams as shown in Fig. 4. The theoretical relationships for coefficient of variation ($C_v = S/\overline{U}$) and skewness (γ) of the W2 distribution are obtained solely in terms of the shape parameter β from the following relations [23]:

$$C_v = \frac{\sqrt{\Gamma\left(1+\frac{2}{\beta}\right) - \left(\Gamma\left(1+\frac{1}{\beta}\right)\right)^2}}{\Gamma\left(1+\frac{1}{\beta}\right)}, \tag{66}$$

and

$$\gamma = \frac{\Gamma\left(1+\frac{3}{\beta}\right) - \Gamma\left(1+\frac{1}{\beta}\right)^3}{\left[\Gamma\left(1+\frac{2}{\beta}\right) - \Gamma\left(1+\frac{1}{\beta}\right)^2\right]^{3/2}} - \frac{3\Gamma\left(1+\frac{1}{\beta}\right)\left[\Gamma\left(1+\frac{2}{\beta}\right) - \Gamma\left(1+\frac{1}{\beta}\right)^2\right]}{\left[\Gamma\left(1+\frac{2}{\beta}\right) - \Gamma\left(1+\frac{1}{\beta}\right)^2\right]^{3/2}}. \tag{67}$$

Here moment diagrams are constructed for both synthetic and empirical samples. Fig. 4 illustrates that the coefficient of variation and skewness for synthetic W2 samples with the same n_j, $\hat{\alpha}_j$, and $\hat{\beta}_j$ as the buoy samples closely mimic the W2 theoretical relationship, whereas the moments of the actual buoy samples do not. Fig. 4 provides a clear documentation of how poorly the tail behavior of the empirical samples is mimicked by the W2 distribution. The scatter about the theoretical relationships in Fig. 4b is shown to arise from real distributional departures alone, and not sampling variability.

While we cannot compare the buoy sample moments and BIW synthetic sample moments to a theoretical BIW moment relationship (because theoretical moment relationships are incalculable for this model), we can compare BIW R^2 values for the buoy samples (from Fig. 3) to BIW R^2 values for synthetic BIW samples. Fig. 5 provides a comparison of the goodness-of-fit of the W2 and BIW distributions to both the real buoy samples and the synthetic buoy samples. For each real buoy sample, we randomly generate 2 synthetic samples: one from the W2 model and one from the BIW model. We use the same parameters and sample sizes as the actual samples, and then fit the two distributions to their respective synthetic samples using the same parameter estimation methods described previously. The W2 and BIW models fit the synthetic W2 and BIW samples almost exactly, as expected, with any departures of R^2 values away from 1 reflecting sampling error alone. If the buoy samples truly came from a W2 or BIW parent distribution, they would have R^2 values comparable to those of the W2 or BIW synthetic samples.

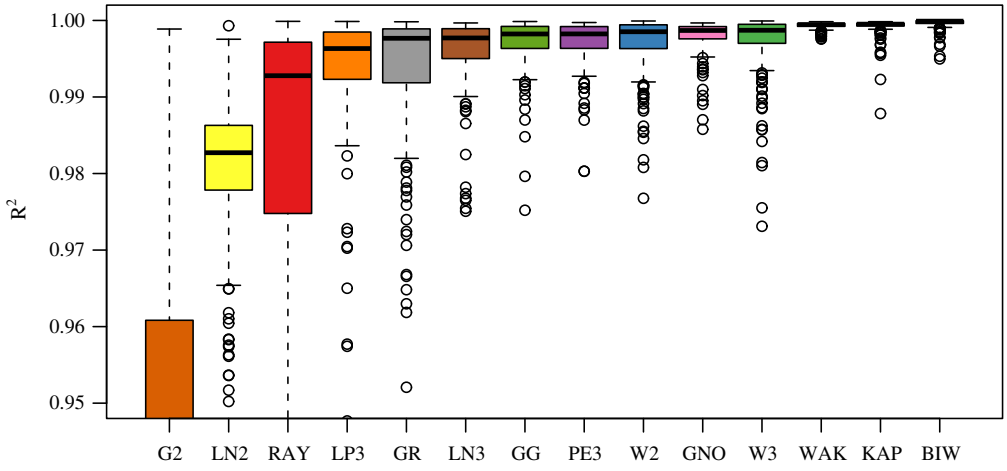

Fig. 3. Boxplots of R^2 values for the distribution fits to the buoy wind speed samples. Distributions are ordered from left to right by ascending median R^2 value (heavy black line in each box).

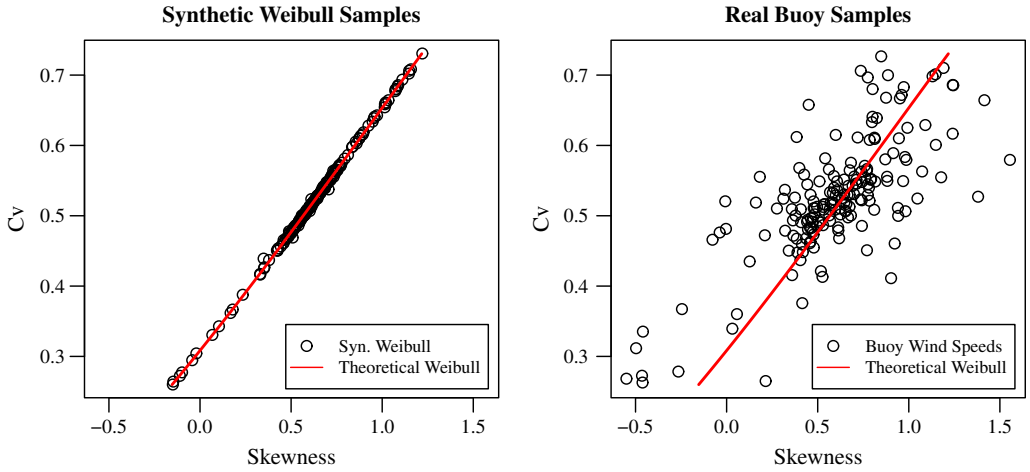

Fig. 4. Comparison of moments between synthetic W2 samples (left) with the real buoy samples (right). The red line represents the theoretical relationship between moments for the W2 distribution. Note the wide dispersion of points around the red line for the buoy samples versus the proximity to the red line that the synthetic samples have. (For interpretation of the references to colour in this figure legend, the reader is referred to the web version of this article.)

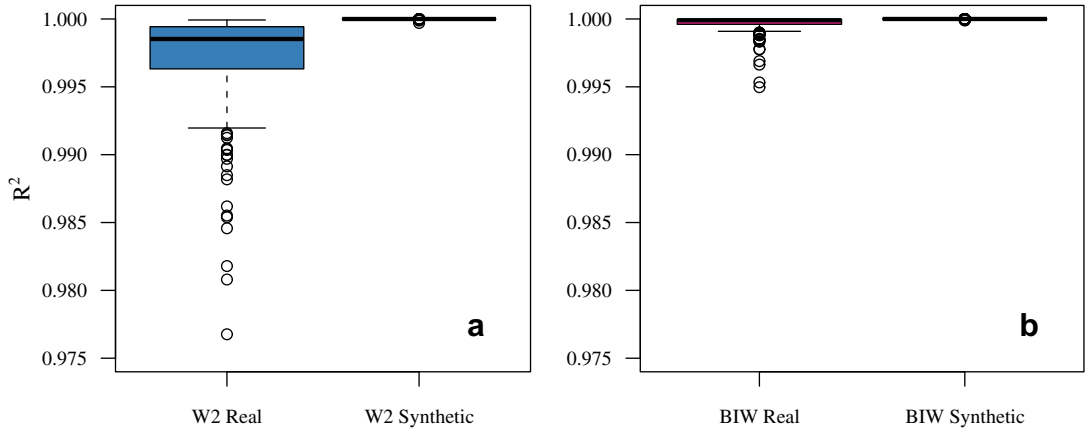

Fig. 5. Boxplots of R^2 values for (a) W2 fits to the real buoy samples (left) and to synthetic samples of same size and parameters (right), and (b) BIW fits to the real buoy samples (left) and to synthetic samples of same size and parameters (right). The greater similarity between the real and synthetic BIW R^2 values (versus those for W2) illustrates that the buoy wind speed samples are better modeled with a BIW distribution.

The departures of the R^2 values from unity for the W2 real samples are much too great to be explained by random sampling error alone (Fig. 5a). The discrepancy between the two boxplots in Fig. 5a results from the inadequacy of the W2 distribution to accurately model the buoy wind speed samples, and cannot be explained by random sampling error. We observe that the BIW model does a much better job at fitting the buoy wind speed samples (Fig. 5b) than the W2 model.

4.2. BIW mixing parameter

Further comparison of the W2 and BIW fits can be found in the mixing parameter ω of the BIW distribution, which tells us about the significance of the second mode in the buoy samples. $\omega = 0.5$ indicates that the two Weibull modes are comparable in size, whereas a value of 1 indicates that no second mode exists. We constrain ω between 0.5 and 1 because we interpret it as the weight of the "strongest" mode in the model. That is, a BIW model with $\omega < 0.5$ can be considered as an alternative model with $\omega_{alt} = 1 - \omega$ and with the shape and scale parameters switched between the two modes (i.e. β_1, α_1, β_2, and α_2 for the initial model respectively become $\beta_{2,alt}$, $\alpha_{2,alt}$, $\beta_{1,alt}$, and $\alpha_{1,alt}$ for the alternative model).

Fig. 6 illustrates the distribution of mixing parameters for the BIW fits to the buoy samples. 68 of the 178 samples have $\omega = 1$, which implies that they follow a W2 distribution. For these 68 samples, any improvement in R^2 from W2 to BIW (e.g. Fig. 7, right-side histogram) only highlights the benefit of using least squares parameter estimation instead of MLE for W2. The remaining samples

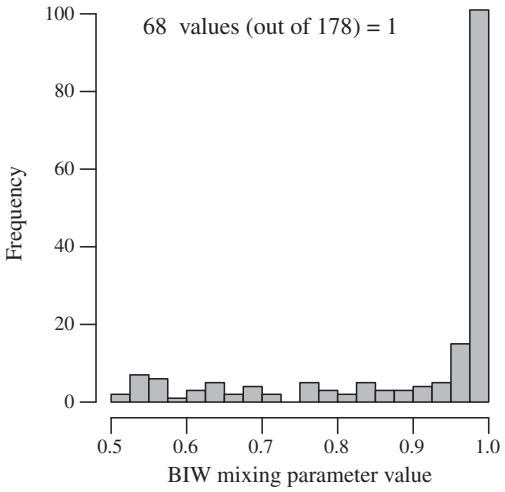

Fig. 6. Distribution of BIW mixing parameters ω from fits to buoy samples. Values of 1 indicate W2 distributed samples.

display a wide range of bimodality, with ω having approximately uniform frequency from 0.5 to 0.95 (Fig. 6). Forty-eight samples have close to 1 (that is $0.95 \leqslant \omega < 1$), indicating diminutive second modes. Thus, a little more than 1/3 of the samples (62 samples) show varying degrees of bimodality ($0.5 \leqslant \omega < 0.95$).

Mapping ω indicates some general spatial structure in the degree of bimodality of the wind speed distributions (Fig. 7; see http://engineering.tufts.edu/cee/geohazards/peopleMorgan.asp for a Google Earth file showing plots for all buoys). We can see that the California coast has a majority of low ω values, where the BIW substantially improves the fit over W2, but higher values of ω also exist in that region. The east coast of North America shows predominantly high values of ω (with little difference between the BIW and W2 fits), with lower values interspersed. Thus, no truly homogenous region exists, and one cannot say for which regions to use which distribution. Therefore, if one is concerned with overall goodness-of-fit, the conservative practice would be to use the BIW as the default wind speed distribution.

4.3. Model performance in terms of average power output

Here we evaluate how well each fitted pdf performs in terms of its ability to agree with the empirical average wind turbine power output computed using

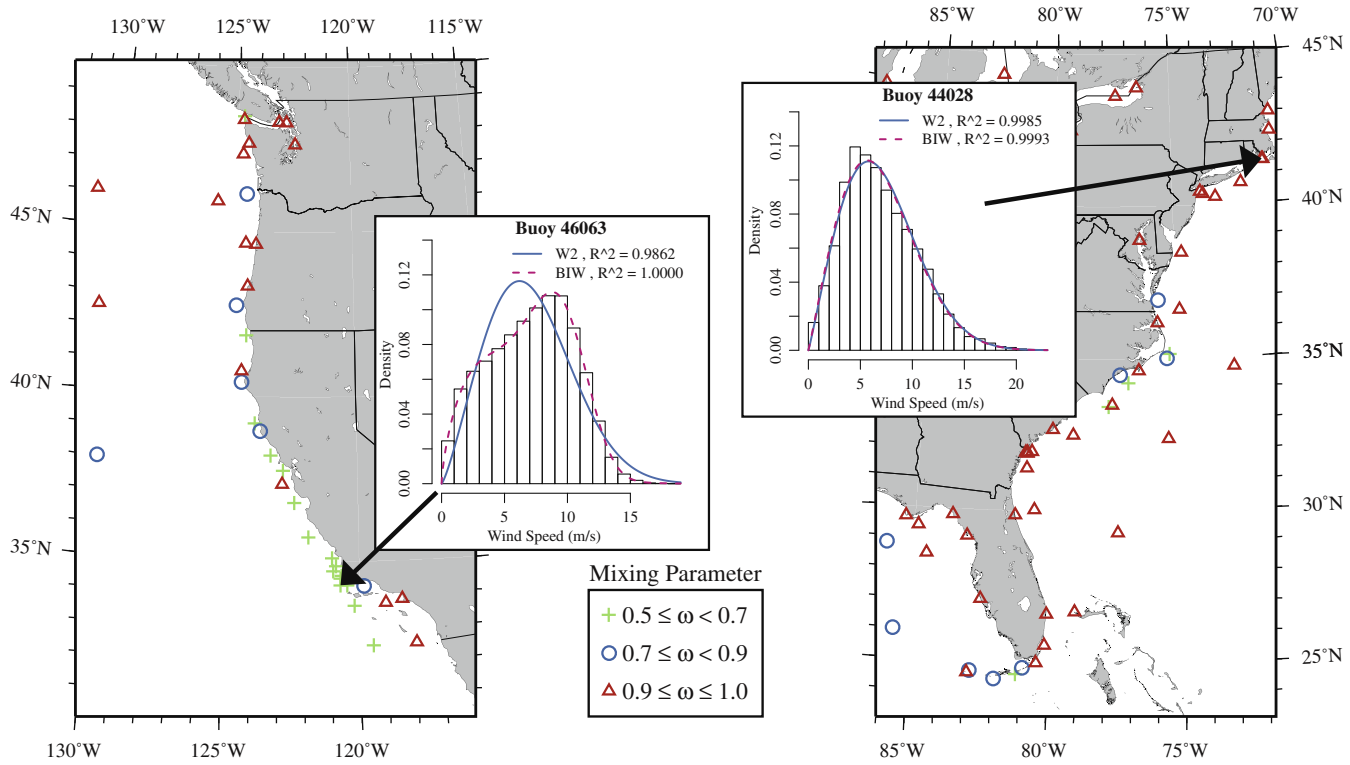

Fig. 7. Map of BIW mixing parameters. Histograms with fitted W2 and BIW distributions exemplify two mixing parameter end-member cases. Left: California sample with a much better fit given by the BIW model ($\omega = 0.53$). Right: Massachusetts buoy data with little difference between W2 and BIW ($\omega = 1$).

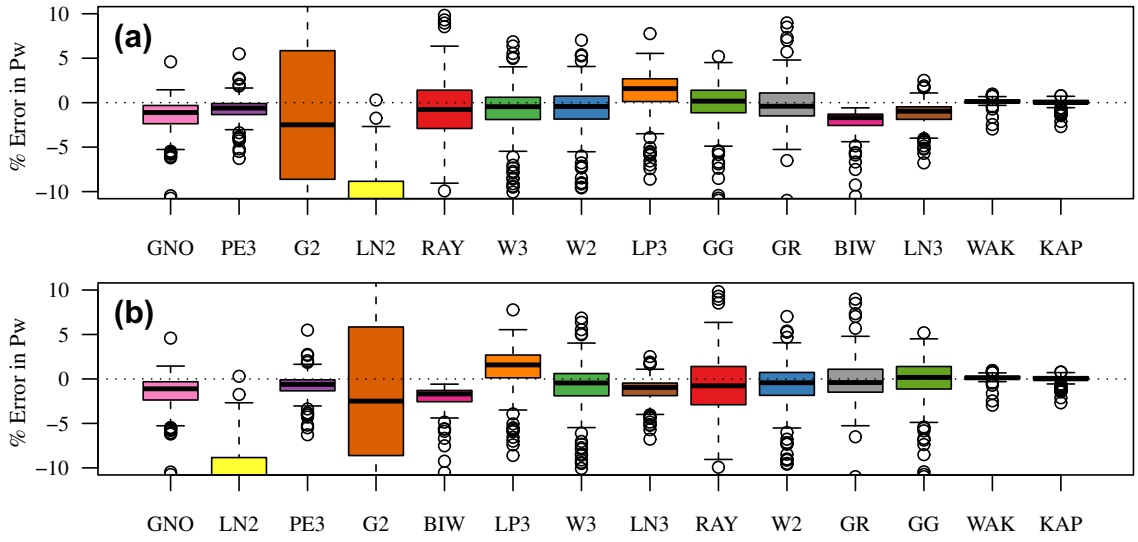

Fig. 8. Boxplots of percent error between time series (empirical) and model-predicted average wind machine power output for each distribution. (a) Ranks by descending mean square error from left to right, and (b) ranks by descending bias.

$$\overline{P}_w = \frac{1}{n}\sum_{i=1}^{n} P_w(U_i) \tag{68}$$

for each buoy sample with size n. The model estimates of the power output $\widehat{\overline{P}}_w$ are obtained from Eq. (1), and we use the regression equation for the Vestas V47-666 KW turbine power curve $P_w(U)$ provided by Chang and Tu [19]. Because turbines do not exist at any of our buoy locations, and because we generally have large samples in this study, we assume the empirical time series estimate as our "true" capacity factor. Chang and Tu [19] find that the time series approach generally estimates capacity factors closer to the actual measured (from the turbines) capacity factors than the distributional approach.

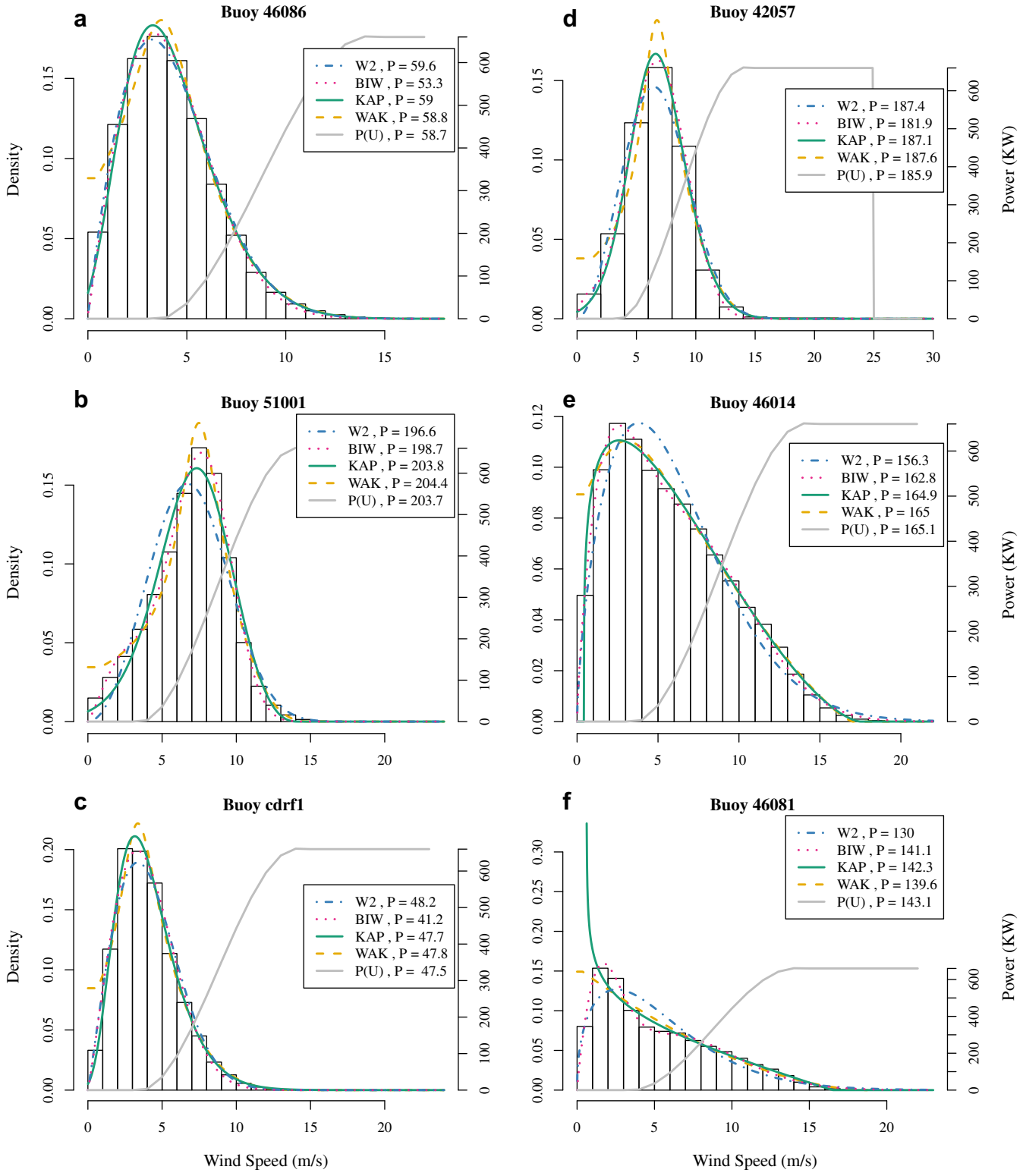

Fig. 9. Histograms with fitted W2, BIW, and WAK pdfs. Power curves $P(U)$ are inserted only to illustrate that higher wind speeds matter most for estimating average power output.

Fig. 8 presents the percent error associated with the average power estimates for all the pdfs considered previously. Here the percent error is defined as

$$\left|\frac{\overline{P}_w - \widehat{\overline{P}}_w}{\overline{P}_w}\right| \times 100\%. \quad (69)$$

Because the power curve weights the influence that probabilities of higher speeds have on $\widehat{\overline{P}}_w$, we see a different performance of the distributions in Fig. 8 than we did in Fig. 3, which ranks based on an unweighted goodness-of-fit to all wind speeds in a sample. In Fig. 8a, we rank the distributions by $MSE = \frac{1}{N}\sum_{j=1}^{N}(\widehat{\overline{P}}_{w,j} - \overline{P}_{w,j})^2$, where $N = 178$ is the number of buoy samples, and in Fig. 8b we rank by bias $= \frac{1}{N}\sum_{j=1}^{N}(\widehat{\overline{P}}_{w,j} - \overline{P}_{w,j})$. Fig. 8 illustrates that the BIW model produces average power estimates with lower MSE than the W2 model (16.8 versus 34.8), but these estimates have more bias (−3.6 versus −1.8). It should be noted here that BIW under-predicts the mean power at every buoy. Also note here that the W2 model does not perform the best out of the 2-parameter models, like it did when comparing R^2. Instead, the GR distribution gives slightly better estimates of average power output than the W2 distribution.

Fig. 8 shows that the KAP distribution yields the least MSE and bias in estimation of mean power output (0.3 and 0.1, respectively), followed closely by the WAK model (0.4 and 0.2). Inspecting the fits of these two distributions to the wind speed histograms in Fig. 9, we begin to understand why the KAP and WAK perform worse than BIW in terms of R^2 and better than BIW in terms of power output. While the BIW provides a good fit to the entire histogram, the KAP and WAK models fit better at the upper tail (i.e., the wind speeds that matter most in $\widehat{\overline{P}}_w$: 4–25 m/s for this power curve), but then diverge from the samples at low wind speeds. The WAK distribution grossly over-predicts the frequency of null wind speeds in every case and sometimes over-predicts the highest density (e.g., Fig. 9a–d). The KAP either over-predicts (Fig. 9a, c and d) or under-predicts (Fig. 9b and e) the peak probability density, and sometimes gives wildly inaccurate null value densities (Fig. 9f), which accounts for some of the lower KAP R^2 values. Thus, the agreement between the models' average power estimates $\widehat{\overline{P}}_w$ and the empirical average power estimates $\overline{P}_w$ depends on how well the models fit the wind speeds between the cut-in and cut-out values (4 m/s and 25 m/s, respectively) of the power curve, and this predictive capability does not necessarily correspond to the models' R^2 values.

4.4. Model performance in terms of extreme wind speeds

In order to evaluate how well the models estimate extreme wind speeds, we compare the number of observations that each model predicts will exceed various percentiles (total exceedances x) to the expected number of exceedances $E[x]$, an analysis based on simple probability theory and previously applied to flood flows [45]. For various low probabilities $p = 1.9 \times 10^{-5}$, 1.9×10^{-6}, 1.9×10^{-7}, we generate model-predicted extreme events from the quantile functions $F^{-1}(1-p)$, where the p is the probability that the event will be exceeded by any observation U_i. We chose these particularly low p values because with such large sample sizes, we want to examine sufficiently rare events. Predicting extreme wind speeds plays an important role in turbine design,

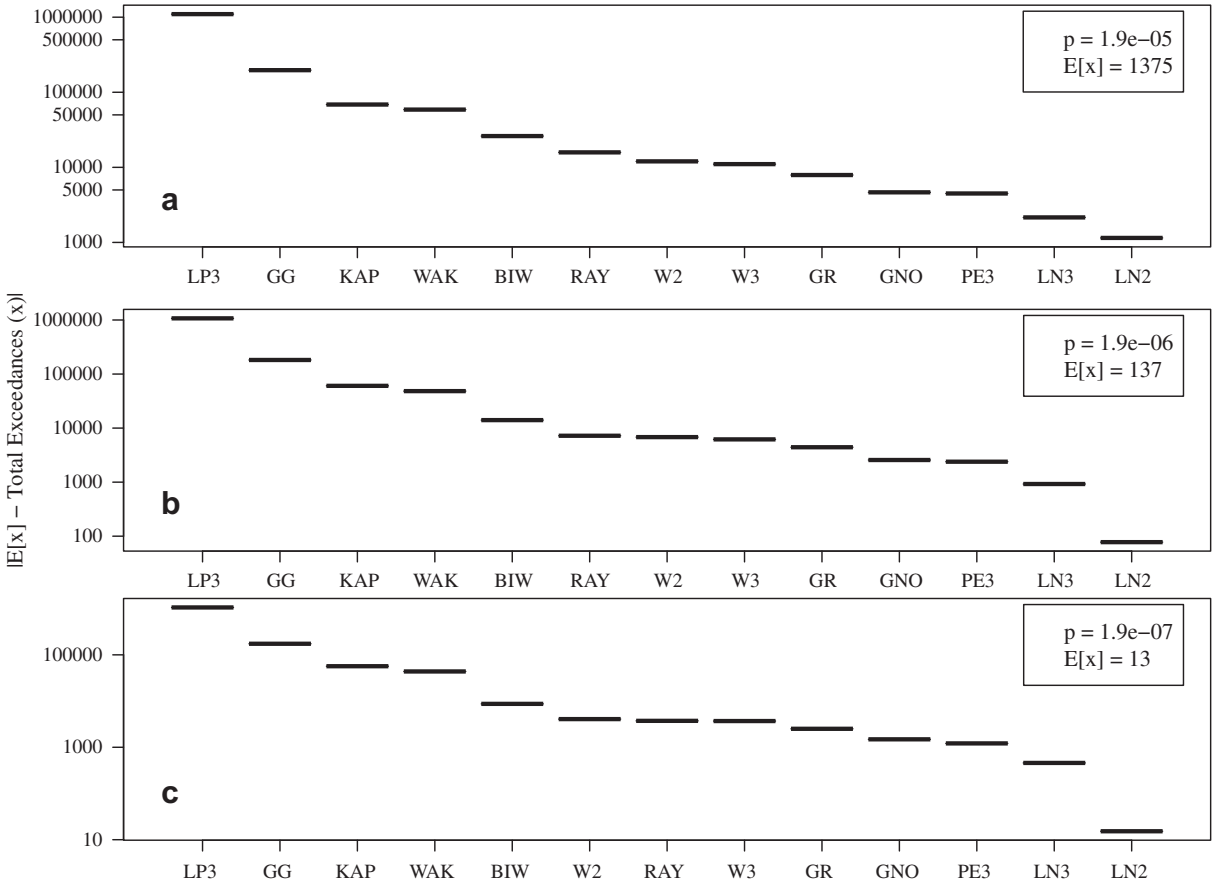

Fig. 10. Total number of observations from all 178 buoys exceeding the $(100 \times p)$th percentile of each fitted distribution. a, b, and c correspond to $p = 1.9 \times 10^{-5}$, 1.9×10^{-6}, 1.9×10^{-7}, respectively. Distributions are ranked from left to right by increasing agreement with $E[x]$ (i.e. decreasing $|E[x] - \text{Total exceedances } (x)|$).

where one normally considers the 50-year return gust value. Traditionally determined via annual maximum data, this extreme gust value can be computed as 1.4 times the 50-year return event determined from the distribution of 10-min mean values [4].

For choosing a suitable model for estimation of extreme design events, such as the wind speed with an average return period of 50 years, we recommend fitting extreme value distributions, such as the Generalized Extreme Value distribution to series of annual maximum wind speeds. We have not considered the prediction of such events here. Instead, in this section, we simply evaluate the ability of various models to capture the extreme tails of 10-min wind speeds. Such analyses can be related to annual frequency analyses and design return period estimation, but we have not addressed those issues here.

We count the number of observations U_i in each sample exceeding the extreme quantiles generated by each model. These quantiles are generated for each sample and each distribution using the fitted parameters from the previous sections. For each distribution, we sum these exceedances over all samples to give the total number of exceedances x used in Fig. 10. The expected number of exceedances is $E[x] = mp$ for each p, where m is the total number of 10-min observations ($\sim$72 million, or $\sim$1376 site-years). Thus, we expect higher wind speed events (lower p) to be exceeded fewer times and correspond to a decrease in $E[x]$.

Fig. 10 compares the absolute difference between the distributions total number of exceedances x and $E[x]$ because the best model for estimating an extreme wind speed from 10-min average data should be in best agreement with $E[x]$. We see that for all p, all distributions perform roughly the same relative to each other, with the LN2 distribution performing the best. However, the errors ($|E[x] - x|$) associated with the LN2 model are still significant (1148, 78, and 15 exceedances, for Fig. 10a, b, and c, respectively; which come out to 83%, 57%, and 115% of their respective $E[x]$ values). Unfortunately, constructing confidence intervals for the estimated number of exceedances as Vogel et al. [45] have done is challenging in our case because our observations cannot be considered independent.

5. Conclusion

In terms of characterizing entire wind speed samples, the BIW, KAP, and WAK distributions offer significantly better fits than other models, with the BIW giving the highest R^2 values. These models are all quite complex, with each having 4–5 parameters. Considering only the simpler models (2–3 parameters), the traditional W2 distribution generally gives larger R^2 values than all the 2-parameter models, and some of the 3-parameter models. Using many large samples spread over a wide geographic region, we show that the superior fit of the BIW to the data (versus the W2 distribution) cannot be explained by sampling error. BIW synthetic samples more closely resemble the real data than W2 synthetic samples. The BIW model led to better goodness-of-fit than the W2 at all locations, to varying degrees. Mapping the BIW mixing parameter shows the degree to which the BIW differs from the W2 at all locations, and we could not discern any regions showing homogeneity of the mixing parameter.

When predicting power output, the BIW no longer performs as well as other distributions. Because the BIW model does not necessarily model the wind speeds between the cut-in and cut-out values of the power curve as well as the KAP or WAK, it led to considerably greater errors in average wind turbine power output estimates. Among all the models considered, the KAP distribution predicted average power output with the lowest MSE and bias. Interestingly, the LN2 distribution yielded the best estimate of extreme wind speeds, but still exhibited large errors.

The fact that different distributions perform better for different metrics suggests that one's selection of model depends on the wind energy application. While the KAP model best estimates average power output, there may be yet another distribution that is best when estimating fatigue loads, for example. If one's goal is to obtain that distribution which performs best under a particular application, further analyses are needed of the type performed here that validate models based on average power output and extreme wind speed.

Acknowledgements

We thank the Wittich Foundation for supporting this research through the Peter and Denise Wittich Family Fund for Alternative Energy Research at Tufts University. Additional funding was provided by NSF Grant OISE-0530151.

References

[1] US Dept. of Energy, Wind powering America; September 2009. <http://www.windpoweringamerica.gov/>.
[2] Manwell JF, McGowan JG, Rogers AL. Wind energy explained: theory, design and application; 2002.
[3] Lackner MA, Rogers AL, Manwell JF. Uncertainty analysis in MCP-based wind resource assessment and energy production estimation. In: Journal of solar energy engineering – transactions of the ASME: AIAA 45th aerospace sciences meeting and exhibit, vol. 130; 2008.
[4] Burton T, Sharpe D, Jenkins N, Bossanyi E. Wind energy handbook. Wiley; 2001.
[5] Garcia A, Torres JL, Prieto E, Francisco AD. Fitting wind speed distributions: a case study. Solar Energy 1998;62(2):139–44.
[6] Harris RI. Generalised pareto methods for wind extremes. useful tool or mathematical mirage? J Wind Eng Ind Aerodyn 2005;93(5):341–60. doi:10.1016/j.jweia.2005.02.004.
[7] Harris RI. Errors in gev analysis of wind epoch maxima from Weibull parents. Wind Struct 2006;9(3):179–91.
[8] Ramirez P, Carta JA. Influence of the data sampling interval in the estimation of the parameters of the Weibull wind speed probability density distribution: a case study. Energy Convers Manage 2005;46(15–16):2419–38.
[9] Hennessey JP. Some aspects of wind power statistics. J Appl Meteorol 1977;16(2):119–28.
[10] Celik AN. A statistical analysis of wind power density based on the Weibull and Rayleigh models at the southern region of Turkey. Renew Energy 2004;29(4):593–604.
[11] Carta JA, Ramirez P, Velazquez S. Influence of the level of fit of a density probability function to wind-speed data on the WECS mean power output estimation. Energy Convers Manage 2008;49(10):2647–55.
[12] Kiss P, Janosi IM. Comprehensive empirical analysis of ERA-40 surface wind speed distribution over Europe. Energy Convers Manage 2008;49(8):2142–51. doi:10.1016/j.enconman.2008.02.003.
[13] Simiu E, Heckert N, Filliben J, Johnson S. Extreme wind load estimates based on the Gumbel distribution of dynamic pressures: an assessment. Struct Safety 2001;23(3):221–9.
[14] Jaramillo OA, Borja MA. Wind speed analysis in La Ventosa, Mexico: a bimodal probability distribution case. Renew Energy 2004;29(10):1613–30.
[15] Akpinar S, Akpinar EK. Estimation of wind energy potential using finite mixture distribution models. Energy Convers Manage 2009;50(4):877–84.
[16] Carta JA, Ramirez P. Use of finite mixture distribution models in the analysis of wind energy in the Canarian Archipelago. Energy Convers Manage 2007;48(1):281–91.
[17] Carta JA, Ramirez P, Velazquez S. A review of wind speed probability distributions used in wind energy analysis Case studies in the Canary Islands. Renew Sustain Energy Rev 2009;13(5):933–55.
[18] Carta JA, Ramirez P. Analysis of two-component mixture Weibull statistics for estimation of wind speed distributions. Renew Energy 2007;32(3):518–31.
[19] Chang T-J, Tu Y-L. Evaluation of monthly capacity factor of WECS using chronological and probabilistic wind speed data: a case study of Taiwan. Renew Energy 2007;32(12):1999–2010.
[20] NDBC. Noaa's national data buoy center; 2009. <http://www.ndbc.noaa.gov/> [07.01.09].
[21] IEC. Wind turbines – part 1: design requirements. Tech. rep. 61400-1 Ed.3, International Electrotechnical Commission; 2005.
[22] Krishnamoorthy K. Handbook of statistical distributions with applications. New York: Chapman & Hall; 2006.
[23] Murthy DNP, Xie M, Jiang R. Weibull models 2004.
[24] Kundu D, Raqab M. Generalized Rayleigh distribution: different methods of estimations. Comput Stat Data Anal 2005;49(1):187–200. doi:10.1016/j.csda.2004.05.008.
[25] Stewart DA, Essenwanger OM. Frequency-distribution of wind speed near-surface. J Appl Meteorol 1978;17(11):1633–42.

[26] Cohen AC. Multi-censored sampling in 3 parameter Weibull distribution. Technometrics 1975;17(3):347–51.
[27] Kaminsky FC. Four probability densities (log-normal, gamma, Weibull, and Rayleigh) and their application to modelling average hourly wind speed. In: Proceedings of the international solar energy society; 1977. p. 19.6–19.10.
[28] Stedinger JR. Fitting log normal-distributions to hydrologic data. Water Resour Res 1980;16(3):481–90.
[29] Hosking J, Wallis J. Regional frequency analysis: an approach based on L-moments. Cambridge University Press; 1997.
[30] Sherlock RH. Analyzing winds for frequency and duration. Meteorol Monogr 1951;1:42–9.
[31] Auwera L, Meyer F, Malet L. The use of the Weibull three-parameter model for estimating mean wind power densities. J Appl Meteorol 1980;19:819–25.
[32] Putnam PC. Power from the wind. New York: D. Van Nostrand Company, Inc.; 1948.
[33] Griffis VW, Stedinger JR. Log-Pearson type 3 distribution and its application in flood frequency analysis. II: parameter estimation methods. J Hydrol Eng 2007;12(5):492–500.
[34] Hirose H. Maximum likelihood parameter estimation in the three-parameter gamma distribution. Comput Stat Data Anal 1995;20(4):343–54.
[35] Stacy EW, Mihram GA. Parameter estimation for a generalized Gamma distribution. Technometrics 1965;7(3):349–58.
[36] Houghton JC. Birth of a parent – Wakeby distribution for modeling flood flows. Water Resour Res 1978;14(6):1105–9.
[37] Vogel RM, Mcmahon TA, Chiew FHS. Floodflow frequency model selection in Australia. J Hydrol 1993;146(1–4):421–49.
[38] Guttman NB, Hosking JRM, Wallis JR. Regional precipitation quantile values for the continental United States computed from L-moments. J Climate 1993;6(12):2326–40.
[39] Landwehr JM, Matalas NC, Wallis JR. Estimation of parameters and quantiles of Wakeby distributions. 1. Known lower bounds. Water Resour Res 1979;15(6):1361–72.
[40] Landwehr JM, Matalas NC, Wallis JR. Estimation of parameters and quantiles of Wakeby distributions. 2. Unknown lower bounds. Water Resour Res 1979;15(6):1373–9.
[41] Hosking JRM. Fortran routines for use with the method of L-moments, version 3. Research report RC 20525, IBM Research Division; 1996.
[42] Asquith WH. Lmomco: L-moments, trimmed L-moments, L-comoments, and many distributions, R package version 0.96.3; 2009.
[43] R Development Core Team. R: a language and environment for statistical computing, R Foundation for Statistical Computing, Vienna, Austria; 2009. <http://www.R-project.org>.
[44] Ramirez P, Carta JA. The use of wind probability distributions derived from the maximum entropy principle in the analysis of wind energy: a case study. Energy Convers Manage 2006;47(15–16):2564–77.
[45] Vogel RM, Thomas WO, Mcmahon TA. Flood-flow frequency model selection in Southwestern United States. J Water Resour Plan Manage – ASCE 1993;119(3):353–66.